ARCHIVES OF ACOUSTICS
14, 1-2, 29-43 (1989)

ACOUSTICAL SHADOW OF A SPHERE IMMERSED IN WATER. I

LESZEK FILIPCZYŃSKI, TAMARA KUJAWSKA

Department of Ultrasonics, Institute of Fundamental Technological Research,
Polish Academy of Sciences

(00-049 Warszawa, ul. Świętokrzyska 21)

In this study the acoustical field behind a rigid sphere is determined for the incidence of a plane harmonic wave on it. This field was determined as the sum of acoustic pressures of the wave incident on the sphere and reflected from it. Formulae describing the reflected wave pressure given in different form by American, Japanese and Soviet acousticians, were compared and their identity demonstrated. It was shown, that these formulae, though valid for fixed spheres, can in practical hydroacoustic cases be also used for movable spheres. On this basis directional characteristics of the shadow behind the sphere were determined for the values of $ka = 100\pi$, 40π, 20π and 8π, which are essential for hydroacoustic problems and for ultrasonic medical diagnostics. These characteristics were determined for distances falling between 10 a and 100 a, where a denotes the radius of the sphere. Moreover, the shape of directional characteristics was interpreted and the ranges of the shadow were determined for different values of ka.

W pracy wyznaczono pole akustyczne za sztywną kulą, powstające w stanie ustalonym przy padaniu na nią płaskiej fali harmonicznej. Pole to wyznaczono jako sumę ciśnienia fali padającej na kulę i ciśnienia fali od niej odbitej. Porównano wzory opisujące pole ciśnienia fali odbitej, podane w różnych postaciach przez akustyków amerykańskich, japońskich i radzieckich wykazując ich identyczność. Pokazano, że wzory te, choć słuszne dla kul nieruchomych, mogą w praktycznych przypadkach hydroakustyki być również stosowane dla kul swobodnych. Na tej podstawie wyznaczono charakterystyki kierunkowe cienia za kulą dla iloczynów liczby falowej k i promienia kuli a, $ka = 100\pi$, 40π 20π i 8π, istotnych w problematyce hydroakustycznej i ultradźwiękowej diagnostyce medycznej. Charakterystyki te, zmieniające się w zależności od odległości za kulą wyznaczono dla odległości zawartych w granicach od 10 a do 1000 a z krokiem kątowym równym 1°, 0,2° lub 0,05°. Podano przy tym interpretację kształtu tych charakterystyk oraz wyznaczono zasięgi strefy cienia dla różnych wartości ka.

1. Introduction

The problem of acoustical shadow behind solid bodies is essential for many questions of the ultrasonic technique, in particular for hydroacoustics and medical diagnostics. In the literature, many studies were devoted to wave reflection from

solid bodies, such as sphere, cylinder etc. On the other hand, the authors did not come across studies related to analysis of the shadow forming behind such solid bodies.

The object of the study is the acoustical shadow forming in the steady state behind a rigid sphere immersed in water. The obtained results can be also generalized to soft tissues since they contain more than 70% of water in their composition and their acoustical parameters are very close to those of water. The previous rather preliminary, studies by the authors [3] showed that the shadow characteristics for rigid and elastic spheres resemble each other. It was assumed, therefore, that the considered spheres are rigid. The computer time necessary for the determination of the shadow behind an elastic sphere is much longer than in the case of a rigid sphere. Moreover, this applies to homogeneous and isotropic elastic spheres, and after all, in hydrolocation practice or in medical diagnostics the inner structure of solid bodies is very complex and unknown *a priori*.

2. Wave reflection from fixed and free movable spheres

Considering the ultrasonic wave reflection from a sphere, it is necessary to distinguish between two cases: the case of a movable sphere, which can freely move in water, and that of a fixed sphere. In real sea conditions, spherical objects can be free, i.e., moving under the effect of the incident wave. This case can be considered on the basis of the result of study [9].

Between the amplitude of the harmonic plane wave of the acoustic pressure p_i incident on the sphere and the amplitude of the wave p_r reflected from the sphere, there is a relation which takes the following form for a distance which is large compares with the sphere radius and the wave-length [8]

$$p_r = \frac{a}{2r} f_\infty(ka) p_i \tag{1}$$

where a is the sphere radius, $k = \omega/c$, c is the wave velocity in water, r is the distance from its centre. The function $f_\infty(ka)$ is called the form function and depends in general on mechanical parameters of the sphere and the ambient medium. Using the complex formulae given in papers [8] and [7] it is possible to determine the function $f_\infty(ka)$ for both rigid and elastic spheres. However, the theory and the formulae derived on its grounds apply only to fixed spheres.

The above-mentioned authors [9] introduced a correction to the function $f_\infty(ka)$ which permits the use of Eq. (1) for rigid movable spheres too. Then, for movable spheres there is the modified form function in the form

$$f_\infty^M(ka) = f_\infty(ka) + \Delta f_\infty(ka), \tag{2}$$

where

$$\Delta f_\infty(ka) = \frac{6j}{ka}\left[\frac{\xi ka j_1'(ka) - j_1(ka)}{\xi ka h_1^{(2)\prime}(ka) - h_1^{(2)}(ka)} - \frac{j_1'(ka)}{h_1^{(2)\prime}(ka)}\right], \tag{3}$$

j_1 and j_1' are the spherical Bessel function of the first order and its derivative with respect to the argument. $h_1^{(2)}$ and $h_1^{(2)\prime}$ are spherical Hankel functions of the second kind, of the first order and its derivative with respect to the argument, $j = \sqrt{-1}$, ξ is the density ratio between the sphere and the ambient liquid.

Fig. 1 shows the modified shape function (modulus) calculated by the authors for a free movable sphere with density $\xi = 7.7$ g/cm^3 steel and for a fixed rigid sphere (curve R). The curve R does not depend on the density of the sphere.

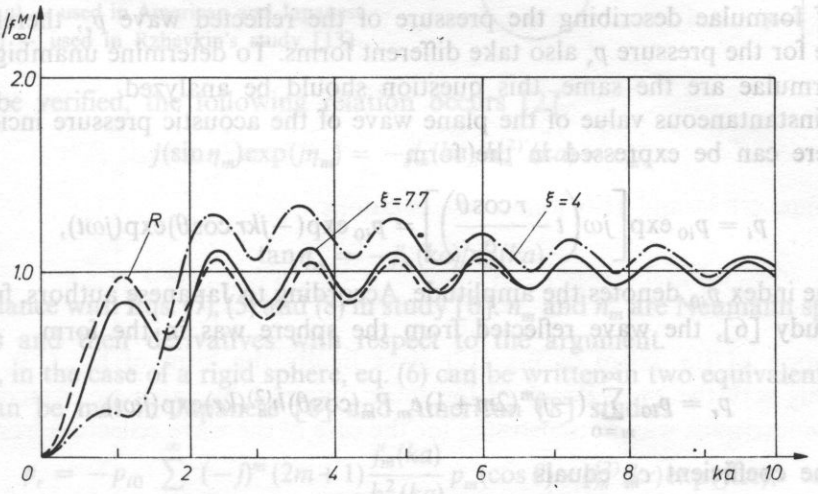

FIG. 1. The modulus of the shape function $f_\infty(ka)$ for a fixed rigid sphere (R) and the modified shape function ka for a free movable sphere with the relative density $\xi = 7.7$ (steel) and $\xi = 4$

Hence, for $ka > 6$, both curves, namely the curve R and that for steel ($\xi = 7.7$) practically coincide. On the other hand, for small values of ka, there can be large differences between the two curves (e.g. curve $\xi = 4$). Hence, it can be concluded that in the present case a sphere with large density can be treated as a fixed one. In practical cases in echo ranging this condition is usually satisfied. On the other hand the conclusion is not valid for spheres with small density and for low values of ka since, then the rigid sphere vibrates as a whole under the action of the incident wave pressure. In such a case verifying calculations should be performed according to Eqs. (2) and (3).

3. Acoustical shadow. Formulae describing wave reflection from a rigid sphere in steady state

The shadow forming arround a rigid sphere can be determined from expressions describing the acoustic pressure of the wave p_s emerging around the sphere. It is the sum of acoustic pressures of the plane wave incident on the sphere p_i and of the reflected wave p_r

$$p_s = p_i + p_r. \tag{4}$$

The acoustic pressure of the wave reflected from the sphere p_r is obtained as a result of the solution of the scalar wave equation in the medium surrounding the sphere. The boundary condition should be satisfied, namely the normal component of the acoustic velocity should vanish on the surface of the rigid sphere.

Since in the studies by American, Japanese and Soviet authors there are various forms of formulae describing the pressure of the reflected wave p_r, therefore the formulae for the pressure p_s also take different forms. To determine unambigously if these formulae are the same, this question should be analyzed.

The instantaneous value of the plane wave of the acoustic pressure incident on the sphere can be expressed in the form

$$p_i = p_{i0} \exp\left[j\omega\left(t - \frac{r\cos\theta}{c}\right)\right] = p_{i0} \exp(-jkr\cos\theta)\exp(j\omega t), \tag{5}$$

where the index p_{i0} denotes the amplitude. According to Japanese authors, from Eq. (3) in study [6], the wave reflected from the sphere was in the form

$$p_r = p_{i0} \sum_{m=0}^{\infty} (-j)^m (2m+1) c_m P_m(\cos\theta) h_m^{(2)}(kr) \exp(j\omega t), \tag{6}$$

where the coefficient c_m equals

$$c_m = -[F_m j_m(ka) - kaj'_m(ka)]/[F_m h_m^{(2)}(ka) - kah_m^{(2)'}(ka)]. \tag{7}$$

Formulae (5) and (6) are valid in a polar coordinate system in which the wave is incident on the sphere travelling from left to right (Fig. 2 a). In this system the radius was denoted by r and the azimuth by θ. $P_n(\cos\theta)$ denotes the Legendre polynomial and $h_m^{(2)}$ and $h_m^{(2)'}$ are spherical Hankel functions of the second kind and its derivative with respect to the argument.

It can be shown [2] for a rigid sphere that

$$F_m = 0. \tag{8}$$

Then, Eq. (7) becomes

$$c_m = -j'_m(ka)/h_m^{(2)'}(ka). \tag{9}$$

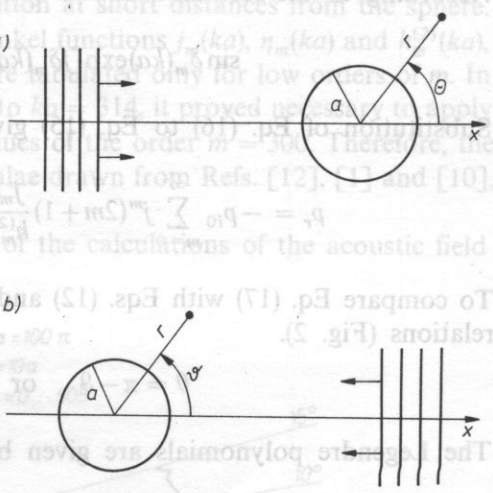

FIG. 2. The polar coordinate system and the direction of the incidence of the plane wave on the sphere. a) – used in American and Japanese studies, b) – used in Rzhevkin's study [13]

As can be verified, the following relation occurs [2]

$$j(\sin\eta_m)\exp(j\eta_m) = -j'_m(ka)/h_m^{(2)'}(ka) = c_m, \tag{10}$$

where

$$\tan\eta_m = -j'_m(ka)/n'_m(ka) \tag{11}$$

in accordance with Eqs. (7), (5) and (8) in study [6]. n_m and n'_m are Neumann spherical functions and their derivatives with respect to the argument.

Thus, in the case of a rigid sphere, eq. (6) can be written in two equivalent forms, which can be met in Japanese [6] and American [8] studies

$$p_r = -p_{i0}\sum_{m=0}^{\infty}(-j)^m(2m+1)\frac{j'_m(ka)}{h_m^2(ka)}p_m(\cos\theta)\times h_m^{(2)}(kr)\exp(j\omega t), \tag{12}$$

and

$$p_r = -p_{i0}\sum_{m=0}^{\infty}(-j)^{m+1}(2m+1)\sin\eta_m\exp(j\eta_m)P_m(\cos\theta)h_m^{(2)}(kr)\exp(j\omega t), \tag{13}$$

where $\tan\eta_m$ is expressed by Eq. (11). The above formulae are valid in the coordinate system r, θ (Fig. 2a). On the other hand in Soviet studies there are different formulae [12]. To compare them with the formulae of Japanese and American authors, let us introduce the coordinate system r, ϑ, in which the wave incident on the sphere travels from right to left (Fig. 2 b). It has the form (see [12], p. 257).

$$p_i = p_{i0}\exp\left[j\omega\left(t+\frac{r\cos\vartheta}{c}\right)\right] = p_{i0}\exp(jkr\cos\vartheta)\exp(j\omega t). \tag{14}$$

In turn, from Eq. (9.6) in the cited handbook [12], the wave reflected from the sphere is described by the formula

$$p_r = -p_{i0}\sum_{m=0}^{\infty}j^{m+1}(2m+1)\sin\delta_m(ka)\exp[j\delta_m(ka)]P_m(\cos\vartheta)h_m^{(2)}(kr)\exp(j\omega t). \tag{15}$$

According to the formulae in Ref. [12] (p. 259) for a rigid sphere

$$\sin\delta_m(ka)\exp[j\delta_m(ka)] = j[j'_m(ka)/h_m^{(2)\prime}(ka)]. \tag{16}$$

Substitution of Eq. (16) to Eq. (15) gives

$$p_r = -p_{i0}\sum_{m=0}^{\infty} j^m(2m+1)\frac{j'_m(ka)}{h_m^{(2)}(ka)}P_m(\cos\vartheta)h_m^{(2)}(kr)\exp(j\omega t). \tag{17}$$

To compare Eq. (17) with Eqs. (12) and (13) one should notice that the following relations (Fig. 2).

$$\theta = \pi - \vartheta \quad \text{or} \quad \cos\theta = -\cos\vartheta. \tag{18 a, b}$$

The Legendre polynomials are given by the expression [1]

$$P_m(x) = \frac{1}{2^m m!}\frac{d^m[(x^2-1)^m]}{dx^m}. \tag{19}$$

From Eqs. (18 b) and (19) follow the relations

$$P_m(x) = (-1)^m P_m(-x) \quad \text{or} \quad P_m(\cos\vartheta) = (-1)^m P_m(\cos\theta). \tag{20 a, b}$$

Substitution of Eq. (20 b) in Eq. (17) gives finally the form of Eq. (12).

In this way the equivalency of formulae obtained by Japanese, American and Soviet acousticians was demonstrated for the case of the wave reflection from a rigid sphere.

4. Directional characteristics of the shadow

Taking into account relations (4), (5) and (13) computer programmes elaborated from the following formula (assuming $p_{i0} = 1$) were applied for calculations of the shadow behind a rigid sphere

$$p_s = \exp(-jkr\cos\theta) - \sum_{m=0}^{\infty}(-j)^{m+1}(2m+1)\sin\eta_m(ka)\exp[j\eta_m(ka)]P_m(\cos\theta)h_m^{(2)}(kr) \tag{21}$$

where the quantity $\eta_m(ka)$ is given by Eq. (11). Eqs. (12), (13) and (21) can be simplified if the spherical Hankel function $h_m(kr)$ is replaced by approximating

formulae valid for large arguments kr. However, this simplification was abandoned in order to investigate the shadow distribution at short distances from the sphere.

The spherical Bessel, Neumann and Hankel functions $j_m(ka)$, $\eta_m(ka)$ and $h_m^{(2)}(ka)$, and also Legendre polynomials $P_m(\cos\theta)$ are tabulated only for low orders of m. In the present study, for large values of ka up to $ka = 314$, it proved necessary to apply the above mentioned functions even to values of the order $m = 300$. Therefore, the computations involved the reduction formulae drawn from Refs. [12], [1] and [10], and appropriate computer programmes.

Fig. 3, 4, 5 and 6 show chosen results of the calculations of the acoustic field

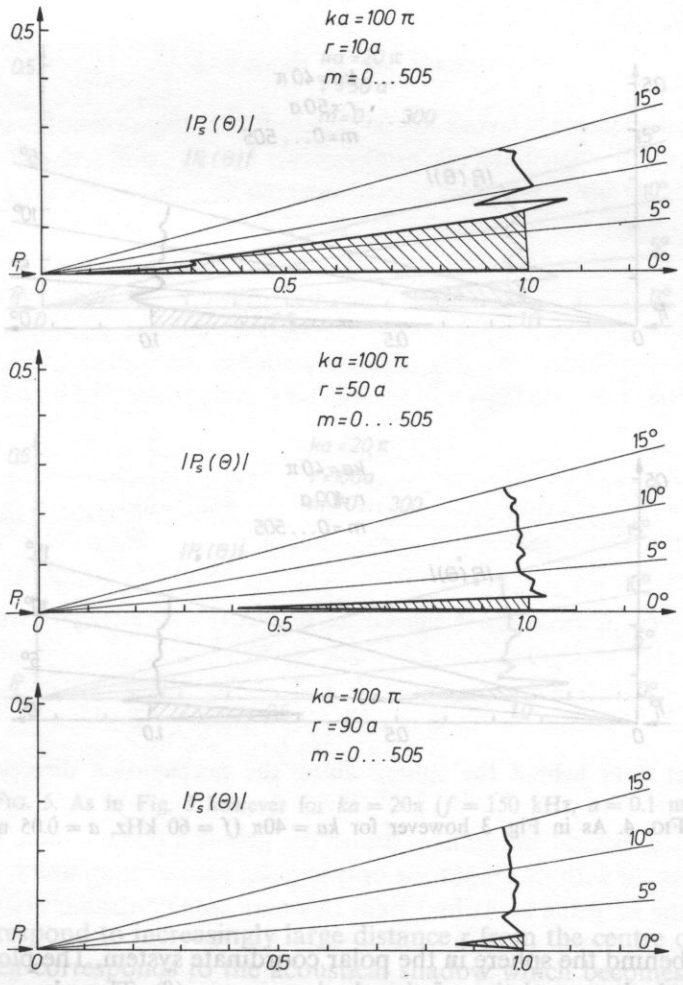

FIG. 3. Directional characteristics of the acoustic field behind the sphere for $ka = 100\pi$ ($f = 150$ kHz, $a = 0.5$ m) at different distances r. The dashed area corresponds to the shadow

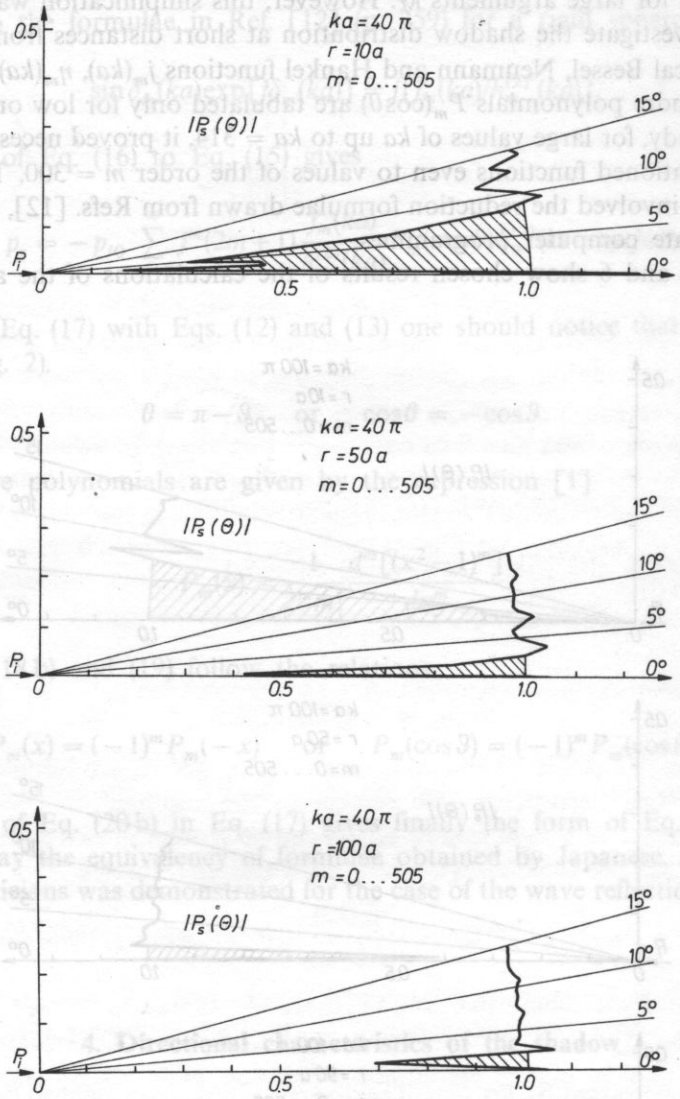

FIG. 4. As in Fig. 3 however for $ka = 40\pi$ ($f = 60$ kHz, $a = 0.05$ m)

distribution behind the sphere in the polar coordinate system. The plotted curves are the directional characteristics of the shadow $p_s = p_s(\theta)$. The plane wave with the amplitude $p_{i0} = 1$ travels from left to right along the axis $\theta = 180°$. The centre of the sphere is situated at the origin of the coordinate system. Successive curves in each of

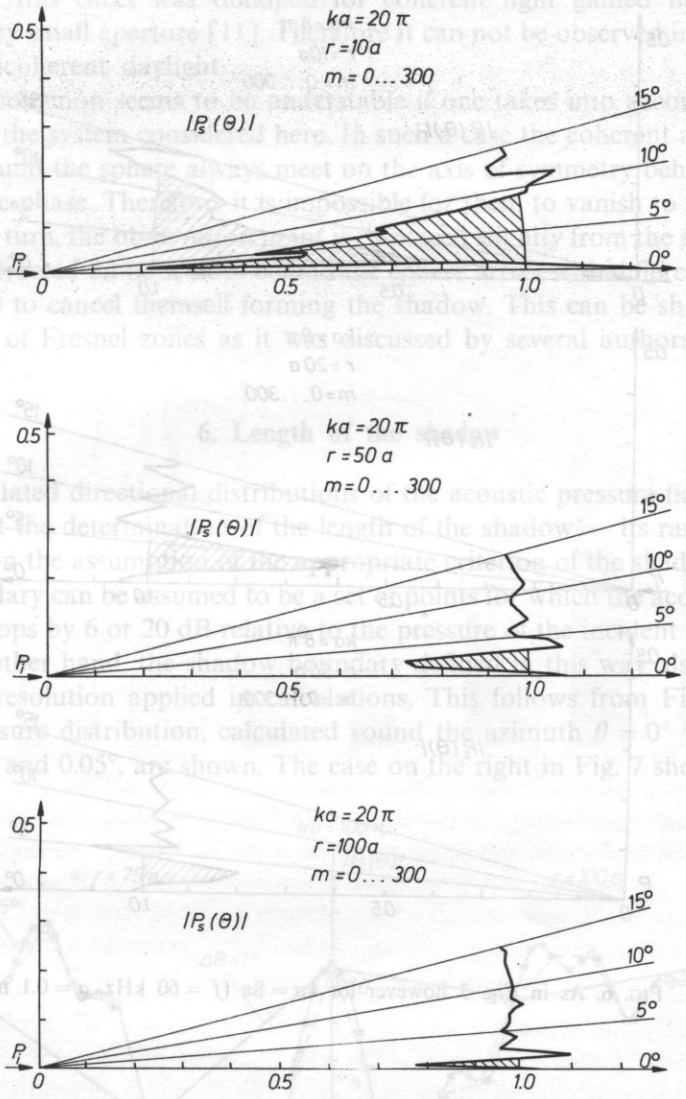

FIG. 5. As in Fig. 3 however for $ka = 20\pi$ ($f = 150$ kHz, $a = 0.1$ m)

the figures correspond to increasingly large distance r from the centre of the sphere. The dashed area corresponds to the acoustical shadow which becomes smaller and smaller as the distance from the sphere increases. The above calculations were carried out for the azimuth step $\Delta\theta = 1°$.

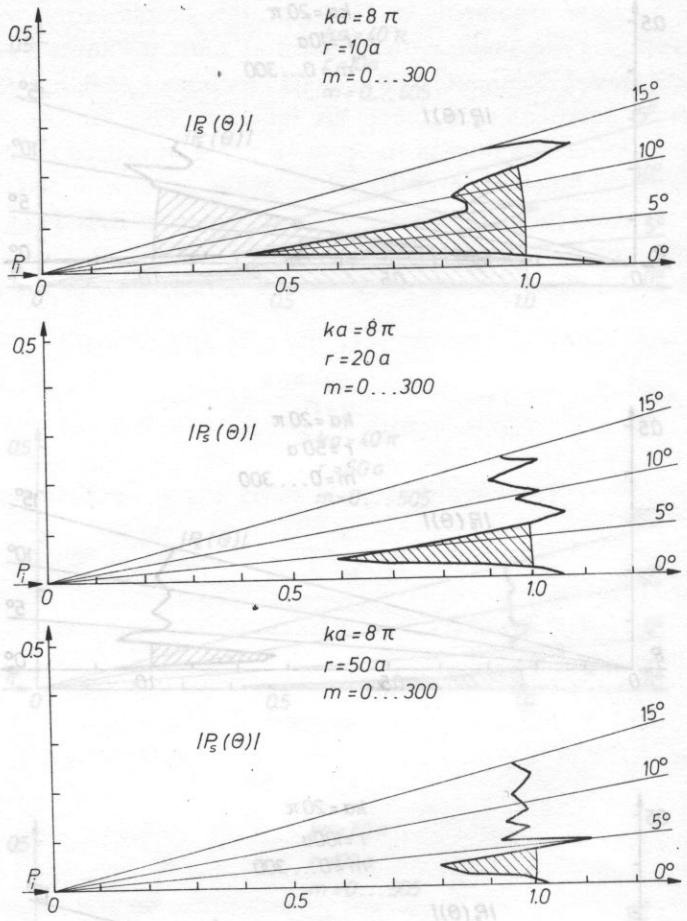

FIG. 6. As in Fig. 3 however for $ka = 8\pi$ ($f = 60$ kHz, $a = 0.1$ m)

5. Acoustical field behind the sphere along the propagation direction of the wave

In all cases, behind the sphere, round the azimuth $\theta = 0°$, there is a thin lobe of acoustic pressure with its amplitude only slightly greater than unity. It is the sharper the greater the ka value is. At first sight this may seen contradictory to our everyday experience with light shadows. However, it was exactly in optics that it was demonstrated experimentally behind an opaque screen, in the centre of its shadow, a bright spot of light [5]. This is evidence to the diffracted of light. This conclusion was drawn by Poisson on the basis of Fresnel's diffraction theory, contributing to the victory of the wave light theory. The conditions of the experiment described in [5]

indicate that this effect was obtained for coherent light gained by letting light through a very small aperture [11]. Therefore it can not be observed in everyday life, in normal incoherent daylight.

This phenomenon seems to be understable if one takes into account the perfect symmetry of the system considered here. In such a case the coherent acoustic waves difracted around the sphere always meet on the axis of symmetry behind the sphere with the same phase. Therefore, it is impossible for them to vanish to form there the shadow. If in turn, the observation point is displaced slightly from the symmetry axis, the waves diffracted on both sides behind the sphere arrive with different phases. It is then possible to cancel themself forming the shadow. This can be shown using the construction of Fresnel zones as it was discussed by several authors [4] and [5].

6. Length of the shadow

The calculated directional distributions of the acoustic pressure field behind the sphere permit the determination of the length of the shadow – its range. However, this depend on the assumption of the appropriate criterion of the shadow boundary. Such a boundary can be assumed to be a set of points for which the acoustic pressure amplitude drops by 6 or 20 dB relative to the pressure of the incident wave pressure p_{i0}. On the other hand, the shadow boundary defined in this way also depends on the angular resolution applied in calculations. This follows from Fig. 7 in which acoustic pressure distribution, calculated round the azimuth $\theta = 0°$ with the steps $\Delta\theta = 1°$, 0.2° and 0.05°, are shown. The case on the right in Fig. 7 shows that if the

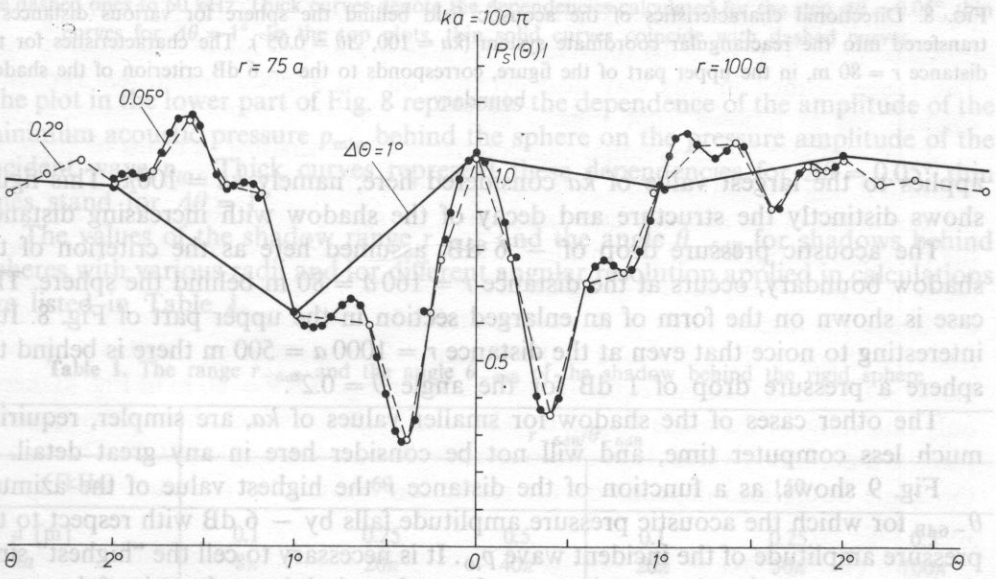

FIG. 7. The acoustic pressure distribution for low angles θ and for $ka = 100\pi$ at the distances $r = 75\,a$ and $r = 100\,a$, calculated with the steps $\Delta\theta = 1°$, 0.2° and 0.05°

criterion of the shadow boundary is set at the level of − 6 dB, the shadow is absent, assuming angular resolution of 1°. For $\Delta\theta = 0.2°$ the shadow becomes distinctly observable, for $\Delta\theta = 0.05°$ no additional changes occur.

Fig. 8 shows the directional characteristics of the acoustic field behind the sphere transfered into the rectangular coordinate system for various distances r. This case

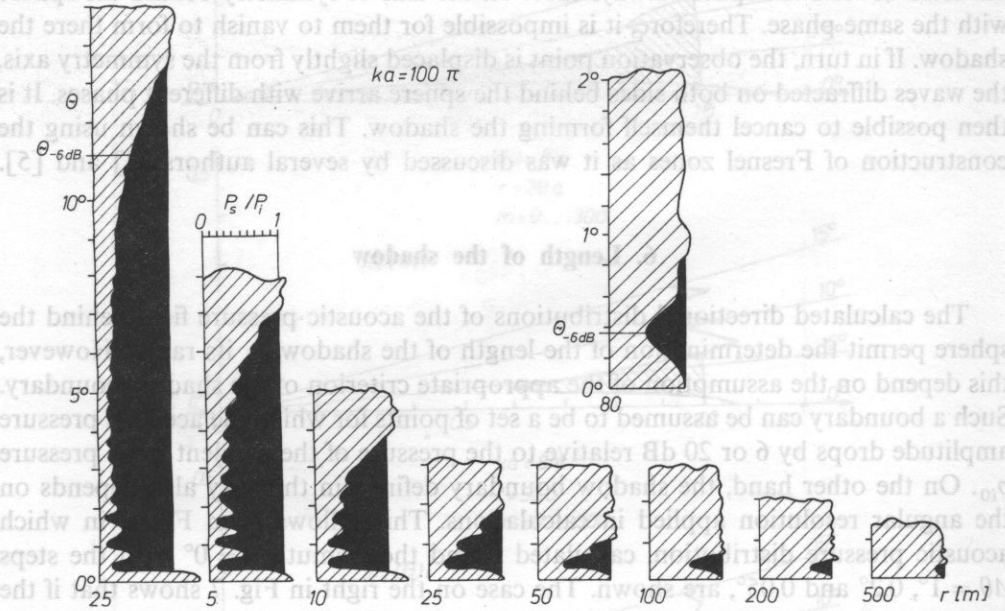

FIG. 8. Directional characteristics of the acoustic field behind the sphere for various distances r, transfered into the reactangular coordinate system ($ka = 100$, $\Delta\theta = 0.05°$). The characteristics for the distance $r = 80$ m, in the upper part of the figure, corresponds to the − 6 dB criterion of the shadow boundary

applies to the largest value of ka considered here, namely $ka = 100\pi$. This figure shows distinctly the structure and decay of the shadow with increasing distance.

The acoustic pressure drop of − 6 dB, assumed here as the criterion of the shadow boundary, occurs at the distance $r = 160\,a = 80$ m behind the sphere. This case is shown on the form of an enlarged section in the upper part of Fig. 8. It is interesting to noice that even at the distance $r = 1000\,a = 500$ m there is behind the sphere a pressure drop of 1 dB for the angle $\theta = 0.2°$.

The other cases of the shadow for smaller values of ka, are simpler, requiring much less computer time, and will not be consider here in any great detail.

Fig. 9 shows, as a function of the distance r the highest value of the azimuth $\theta_{-6\text{dB}}$ for which the acoustic pressure amplitude falls by − 6 dB with respect to the pressure amplitude of the incident wave p_{i0}. It is necessary to cell the "highest" since the second value of such an angle occurs for each main lobe at the axis of the system behind the sphere when the maximum pressure is smaller than − 6 dB (see Fig. 8).

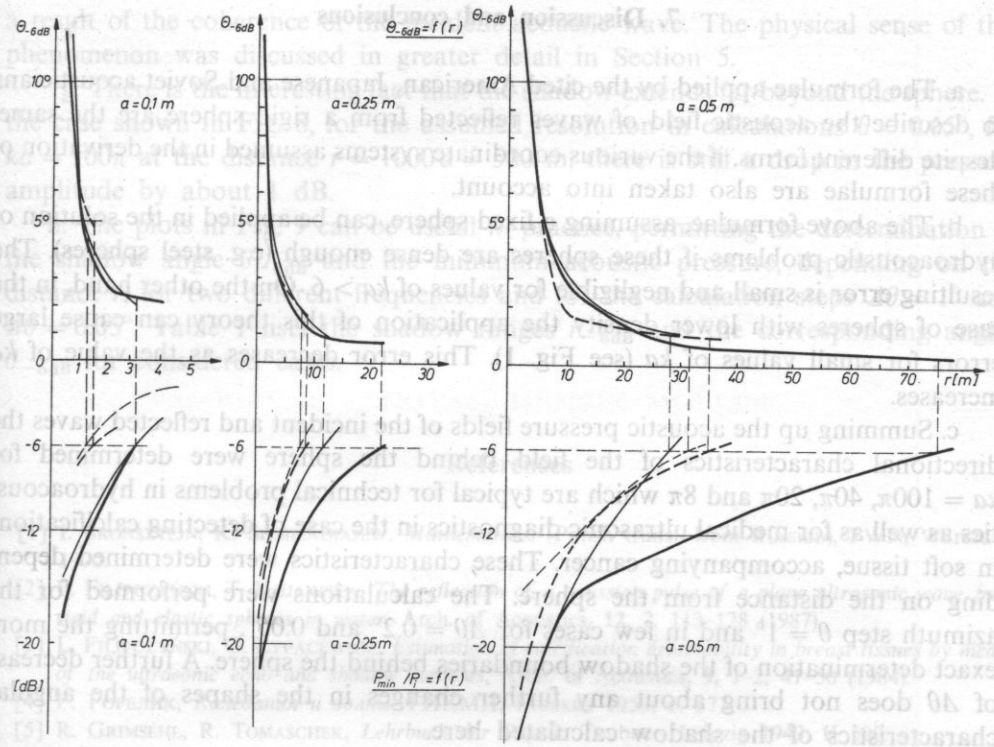

FIG. 9. The dependence of the angle $\theta_{-6\text{dB}}$ and the maximum acoustic pressure $p_{\min}$ behind the sphere on the distance r for three different sphere radius a. Solid curves correspond to the frequency $f = 150$ kHz, the dashed ones to 60 kHz. Thick curves denote the dependencies calculated for the step $\Delta\theta = 0.05°$, thin curves for $\Delta\theta = 1°$. In the top plots, thin solid curves coincide with dashed curves

The plot in the lower part of Fig. 8 represents the dependence of the amplitude of the minimum acoustic pressure $p_{\min}$ behind the sphere on the pressure amplitude of the incident wave p_{i0}. Thick curves represent these dependencies for $\Delta\theta = 0.05°$ thin ones stand for $\Delta\theta = 1°$.

The values of the shadow range $r_{-6\text{dB}}$ and the angle $\theta_{-6\text{dB}}$ for shadows behind spheres with various radii and for different angular resolution applied in calculations are listed in Table 1.

Table 1. The range $r_{-6\text{dB}}$ and the angle $\theta_{-6\text{dB}}$ of the shadow behind the rigid sphere

	$r_{-6\text{dB}}/\theta_{-6\text{dB}}$					
f [kHz]	60			150		
a [m]	0.1	0.25	0.5	0.1	0.25	0.5
ka	8π	20π	40π	20π	50π	100π
$\Delta\theta = 1°$	1.5 m/—	7.5 m/2°	30 m/1°	3 m/2°	12 m/1.2°	28 m/1°
$\Delta\theta = 0.05°$	1.3 m/5°	8.5 m/1.95°	35 m/0.95°	3.5 m/1.95°	22 m/0.76°	75 m/0.35°

7. Discussion and conclusions

a. The formulae applied by the cited American, Japanese and Soviet acousticians to describe the acoustic field of waves reflected from a rigid sphere are the same, despite different forms, if the various coordinate systems assumed in the derivation of these formulae are also taken into account.

b. The above formulae, assuming a fixed sphere, can be applied in the solution of hydroacoustic problems if these spheres are dense enough (e.g. steel spheres). The resulting error is small and negligible for values of $ka > 6$. On the other hand, in the case of spheres with lower density the application of this theory can cause large errors for small values of ka (see Fig. 1). This error decreases as the value of ka increases.

c. Summing up the acoustic pressure fields of the incident and reflected waves the directional characteristics of the field behind the sphere were determined for $ka = 100\pi$, 40π, 20π and 8π which are typical for technical problems in hydroacoustics as well as for medical ultrasonic diagnostics in the case of detecting calcifications in soft tissue, accompanying cancer. These characteristics were determined depending on the distance from the sphere. The calculations were performed for the azimuth step $\theta = 1°$ and in few cases for $\Delta\theta = 0.2°$ and $0.05°$, permitting the more exact determination of the shadow boundaries behind the sphere. A further decrease of $\Delta\theta$ does not bring about any further changes in the shapes of the angular characteristics of the shadow calculated here.

d. To evaluate quantitatively the shadow which decays in a continuous way, it was necessary to introduce a criterion permitting its unambiguous determination. For that purpose the authors proposed the criterion of a drop in the acoustic pressure amplitude by 6 dB relative to the pressure amplitude of the incident wave. The range defined in this way also depends on the angular resolution applied in calculations as follows from Figs. 7 and 9.

e. To evaluate the directional characteristics of the shadow in terms of angle, the azimuth $\theta_{-6\text{dB}}$ was introduced. It is equal to the highest value of the angle for which the amplitude of the acoustic pressure behind the sphere decreases by 6 dB relative to the pressure amplitude of the incident wave. For distances shorter than the shadow range (e.g. for $r = 2.5$ m in Fig. 8), there are two such angles, therefore it is necessary to choose the higher value of them, since there is a still smaller value of θ, resulting from the shape of the main lobe of the directional characteristics, situated near to the axis $\theta = 0°$. For a distance equal to the shadow range (for $r = 80$ m in Fig. 8) there is only one value of the angle $\theta_{-6\text{dB}}$, equal to the angle for which the acoustic pressure reaches a minimum value. In the case considered here this angle is 0, 2°. The value of the angle $\theta_{-6\text{dB}}$ also depends on the resolution assumed in calculations; it follows from Fig. 9.

f. In all the cases of the calculated directional characteristics, there is the main lobe situated round the axis $\theta = 0°$. It is the narrower the greater ka value is. This is

a result of the coherence of the incident acoustic wave. The physical sense of this phenomenon was discussed in greater detail in Section 5.

g. There is the interesting fact that the shadow extends far beyond the sphere. In the case shown in Fig. 8, for the assumed resolution in calculations $\theta = 0.05°$, for $ka = 100\pi$ at the distance $r = 1000\,a = 500$ m, there is still a drop in the pressure amplitude by about 1 dB.

h. The plots in Fig. 9 can be useful in practice, permitting the determination of the shadow angle $\theta_{-6\text{dB}}$ and the minimum acoustic pressure, depending on the distance r, for two different frequencies and for the calculation steps $\Delta\theta = 1°$ and $\Delta\theta = 0.05°$. Table 1 lists the shadow ranges $r_{-6\text{dB}}$ and the corresponding angles $\theta_{-6\text{dB}}$ for considered cases.

References

[1] I. Bronsztejn, K. Siemiendiajew, *Mathemathics* (Polish transl. from Russian), PWN, Warszawa 1970.

[2] L. Filipczyński, T. Kujawska, *The reflection of a gaussian pulse of a plane ultrasonic wave from rigid and elastic spheres in water*, Arch. of Acoustics, **12**, 2, 113–128 (1987).

[3] L. Filipczyński, G. Łypacewicz, *Estimation of calcification detectability in breast tissues by means of the ultrasonic echo and shadow methods*, Arch. of Acoustics, **9**, 1–2, 41–50 (1984).

[4] Г. Горелик, *Колебания и волны*, ГИКМЛ, Москва 1959, с. 371.

[5] R. Grimsehl, R. Tomaschek, *Lehrbuch der Physik*, Teubner, Leipzig 1943, II 590.

[6] T. Hasegawa, Y. Kitagawa, Y. Watanbe, *Sound reflection from an absorbing sphere*, J. Acoust. Soc. Am., **62**, 1298–1300 (1977).

[7] T. Hasegawa, *Comparison of two solutions for acoustic radiation pressure on a sphere*, J. Acoust. Soc. Am., **61**, 6, 1445–1448 (1977).

[8] R. Hickling, *Analysis of echoes from a solid elastic sphere in water*, J. Acoust. Soc. Am., **34**, 1582–1593 (1962).

[9] B. Hickling, N. Wang, *Scattering of sound by rigid movable sphere*, J. Acoust. Soc. Am., 39, 276–280 (1966).

[10] P. Morse, K. Ingard, *Theoretical acoustics*, Mc Graw-Hill, New York 1968.

[11] A. Piekara, Nowe oblicze optyki, PWN, Warszawa 1968, s. 155, (166).

[12] С. Ржевкин, *Курс лекций по теории звука*, ИМУ, Москва 1960.

Received on March 10, 1988.